Bayesian Topological Analysis of Brain Networks

Xukun Zhu[1][0009−0001−2110−4904], Michael W. Lutz[2][0000−0001−8809−5574], and Tananun Songdechakraiwut[3][0009−0008−5637−2811]

[1] Department of Statistical Science, Duke University, USA
[2] Departments of Neurology and Pathology, Duke University School of Medicine, USA
[3] Department of Computer Science, Duke University, USA
songdechakra@wisc.edu

Abstract. Subtle alterations in brain network topology often evade detection by traditional statistical methods. To address this limitation, we introduce a Bayesian inference framework for topological comparison of brain networks that probabilistically models within- and between-group dissimilarities. The framework employs Markov chain Monte Carlo sampling to estimate posterior distributions of test statistics and Bayes factors, enabling graded evidence assessment beyond binary significance testing. Simulations confirmed statistical consistency to permutation testing. Applied to fMRI data from the Duke/UNC Alzheimer's Disease Research Center, the framework detected topology-based network differences that conventional permutation tests were unable to reveal, highlighting its enhanced sensitivity to early or subtle brain network alterations in clinical neuroimaging.

Keywords: Bayesian inference · Persistent homology · Brain networks · fMRI · Alzheimer's disease

1 Introduction

Persistent homology [5] has emerged as a powerful framework for characterizing brain network topology in neurodegenerative diseases, capturing multi-scale network organization through persistence diagrams and Wasserstein distance metrics [9,21]. To statistically compare these topological representations across clinical groups, permutation testing remains the standard approach for group comparisons in neuroimaging, providing non-parametric inference without distributional assumptions [6,17,19]. However, permutation tests yield only binary significance decisions at predetermined thresholds and require computationally intensive resampling for large datasets [12].

Bayesian statistical inference [11] offers a framework that addresses these limitations. By probabilistic modeling of network dissimilarities, Bayesian methods provide complete posterior distributions rather than point estimates, enabling evidence assessment through Bayes factors that quantify the strength of evidence for competing hypotheses and uncertainty quantification via credible intervals [10,14]. While frequently used for network topology inference [1,18],

Bayesian methods are rarely applied to group-level topological testing. However, Bayesian hypothesis tests can match the statistical power of classical permutation tests while providing richer posterior information [16]. Therefore, we propose a Bayesian inference framework to test topological dissimilarities.

The main contributions of this paper are as follows. 1) We present a Bayesian inference framework for comparing brain network topologies that models topological dissimilarities and provides posterior distributions, Bayes factors, and credible intervals. 2) We validate the proposed framework using simulation experiments, confirming it has same statistical power with permutation testing. 3) The method is applied to resting-state fMRI data from the Duke/UNC Alzheimer's Disease Research Center, demonstrating enhanced sensitivity in detecting amyloid and tau pathology-related network alterations compared to permutation testing. The code is publicly available at `https://github.com/XukunZhu-6/Bayesian-Topological-Brain-Networks`.

2 Methods

2.1 Topological Distance and Group Dissimilarity

Each brain network is represented as an undirected, weighted graph derived from functional connectivity. We employ persistent graph homology (PGH), which captures interpretable topological invariants, connected components (0-homology) and independent cycles (1-homology), across the entire range of edge weights using closed-form computation [20]. Given a functional connectivity graph $G = (V, W)$, where V denotes the set of brain regions and $W = \{w_{ij}\}$ represents pairwise functional connections, we define a sequence of binary graphs G_ϵ by applying thresholds to the weights: an edge (i, j) exists in G_ϵ if $w_{ij} > \epsilon$. As ϵ increases, a nested sequence (filtration) of graphs is formed: $G_{\epsilon_0} \supseteq G_{\epsilon_1} \supseteq \cdots \supseteq G_{\epsilon_k}$, where $\epsilon_0 \leq \epsilon_1 \leq \cdots \leq \epsilon_k$ are filtration values.

PGH tracks how topological features emerge and disappear across filtration levels. A feature born at b_l and dying at d_l is represented by a point (b_l, d_l) in a persistence diagram [5]. As ϵ increases, the number of connected components β_0 increases monotonically, while the number of cycles β_1 decreases monotonically. This monotonic behavior ensures that it suffices to record only the birth times of connected components and the death times of cycles: $I_0(G) = \{b_l\}_{l=1}^{|V|-1}, I_1(G) = \{d_l\}_{l=1}^{1+|V|(|V|-3)/2}$. Therefore, we represent the persistence diagram using birth sets for connected components (I_0) and death sets for cycles (I_1).

The topological distance between two networks G_1 and G_2 is defined as the combined Wasserstein distance [3] across graph homology dimensions:

$$\widetilde{W}_{\text{top}}(G_1, G_2) = W_{0D}(G_1, G_2) + W_{1D}(G_1, G_2), \tag{1}$$

where W_{0D} and W_{1D} measure dissimilarity in terms of connected components and cycles. The Wasserstein distance for connected components is defined as: $W_{0D}(G_1, G_2) = \min_{\tau_0} \sum_{b \in I_0(G_1)} \|b - \tau_0(b)\|^2$, where τ_0 is a bijection between

the birth sets $I_0(G_1)$ and $I_0(G_2)$. Similarly, the Wasserstein distance for cycles is defined as: $W_{1D}(G_1, G_2) = \min_{\tau_1} \sum_{d \in I_1(G_1)} \|d - \tau_1(d)\|^2$, where τ_1 is a bijection between the death sets $I_1(G_1)$ and $I_1(G_2)$.

Let $\mathcal{X} = \{X_1, \ldots, X_m\}$ and $\mathcal{Y} = \{Y_1, \ldots, Y_n\}$ denote two groups of brain networks (e.g., Alzheimer's disease patients and healthy controls). We quantify group-level dissimilarity by computing pairwise topological distances between networks. The average within-group distance is defined as:

$$\bar{D}_W = \frac{\sum_{i<j} \widetilde{W}_{\text{top}}(X_i, X_j) + \sum_{i<j} \widetilde{W}_{\text{top}}(Y_i, Y_j)}{\binom{m}{2} + \binom{n}{2}}, \tag{2}$$

which measures the typical topological variability within homogeneous groups. The average between-group distance is:

$$\bar{D}_B = \frac{1}{mn} \sum_{i=1}^{m} \sum_{j=1}^{n} \widetilde{W}_{\text{top}}(X_i, Y_j), \tag{3}$$

reflecting the topological distinction between clinical populations. We use the individual pairwise distances $d_i^{\text{within}} = \widetilde{W}_{\text{top}}(X_a, X_b)$ for all pairs within groups and $d_j^{\text{between}} = \widetilde{W}_{\text{top}}(X_i, Y_j)$ for all cross-group pairs as observed data, rather than the averaged quantities $\bar{D}_W$ and $\bar{D}_B$.

2.2 Bayesian Inference Framework

Let $\mathbf{d}_{\text{w}} = (d_1^{\text{within}}, \ldots, d_{n_{\text{w}}}^{\text{within}})$ and $\mathbf{d}_{\text{b}} = (d_1^{\text{between}}, \ldots, d_{n_{\text{b}}}^{\text{between}})$ denote the vectors of all observed within-group and between-group topological distances derived in Section 2.1, where n_{w} and n_{b} represent the total number of within-group and between-group network pairs, respectively. Given the complete dataset of observed distances $\mathbf{d} = (\mathbf{d}_{\text{w}}, \mathbf{d}_{\text{b}})$, we propose a Bayesian inference framework to quantify uncertainty in group differences.

Wasserstein distances are strictly non-negative and often heavy-tailed. Standard Gaussian models introduce estimation bias by assigning probability to invalid negative values, particularly for high-variance topological features. We therefore employ a Gamma likelihood to capture this intrinsic asymmetry [19]. Correspondingly, we assign Log-Normal priors to the expected distances. This specification enforces parameter non-negativity and naturally accommodates heavy-tailed uncertainty.

We assume each observed distance follows a Gamma distribution parameterized by its mean μ and variance σ^2:

$$d_i^{\text{within}} \sim \text{Gamma}(\mu_{\text{w}}, \sigma_{\text{w}}^2), \quad \text{for } i = 1, \ldots, n_{\text{w}} \tag{4}$$

$$d_j^{\text{between}} \sim \text{Gamma}(\mu_{\text{b}}, \sigma_{\text{b}}^2), \quad \text{for } j = 1, \ldots, n_{\text{b}} \tag{5}$$

where $(\mu_{\text{w}}, \sigma_{\text{w}}^2)$ and $(\mu_{\text{b}}, \sigma_{\text{b}}^2)$ characterize the within-group and between-group distance distributions, respectively. To enforce the physical constraint that expected topological distances must be strictly positive, we assign Log-Normal

Table 1. Validation results comparing permutation testing and Bayesian inference. Experiment 1 tested networks with different structures ($c = 2$ vs $c = 3$), while Experiment 2 tested networks with identical structures ($c = 3$ vs $c = 3$).

Method	**Statistic**	**Exp 1: Different**	**Exp 2: Same**
Permutation Test	Observed ϕ	7.022	0.946
	p-value	< 0.001	0.634
	Decision	Significant	Not Sig.
Bayesian Ratio (ϕ)	Posterior Mean	7.120	0.953
	95% CI	[5.592, 9.261]	[0.734, 1.223]
	$P(\phi > 1)$	1.000	0.330
Bayesian Diff. (Δ)	Posterior Mean	16.156	-0.192
	95% CI	[14.724, 17.585]	$[-1.042, 0.669]$
	$P(\Delta > 0)$	1.000	0.330
Bayes Factor	BF_{10}(LOO)	1.95×10^{139}	6.46×10^{-3}
	Interpretation	Decisive for H_1	Moderate for H_0

priors to the mean parameters. For the variance parameters, we utilize weakly informative Inverse-Gamma priors:

$$\mu_{\mathrm{w}}, \mu_{\mathrm{b}} \sim \mathrm{LogNormal}(-1, 2), \quad \sigma_{\mathrm{w}}^2, \sigma_{\mathrm{b}}^2 \sim \mathrm{InverseGamma}(0.01, 0.01) \tag{6}$$

To test for group differences, we formulate two competing hypotheses. The null hypothesis assumes no topological difference, implying all distances are drawn from a single common Gamma distribution ($\mu_{\mathrm{w}} = \mu_{\mathrm{b}}$). The alternative hypothesis assumes distinct topological structures, where within-group and between-group distances are characterized by distinct parameters ($\mu_{\mathrm{w}} \neq \mu_{\mathrm{b}}$).

By Bayes' theorem, the posterior distribution is $p(\boldsymbol{\theta} \mid \mathbf{d}) \propto p(\mathbf{d} \mid \boldsymbol{\theta}) p(\boldsymbol{\theta})$, where the likelihood factorizes as:

$$p(\mathbf{d} \mid \boldsymbol{\theta}) = \prod_{i=1}^{n_{\mathrm{w}}} \mathrm{Gamma}(d_i^{\mathrm{within}} \mid \mu_{\mathrm{w}}, \sigma_{\mathrm{w}}^2) \prod_{j=1}^{n_{\mathrm{b}}} \mathrm{Gamma}(d_j^{\mathrm{between}} \mid \mu_{\mathrm{b}}, \sigma_{\mathrm{b}}^2) \tag{7}$$

We perform Markov Chain Monte Carlo (MCMC) sampling to obtain S posterior samples $\{\boldsymbol{\theta}^{(s)}\}_{s=1}^{S}$. From these samples, we derive distributions of two test statistics: the ratio $\phi = \mu_{\mathrm{b}}/\mu_{\mathrm{w}}$ measuring relative dissimilarity, which is also used in permutation testing, and the mean difference $\Delta = \mu_{\mathrm{b}} - \mu_{\mathrm{w}}$ quantifying group separation. For each posterior sample s, we compute $\Delta^{(s)} = \mu_{\mathrm{b}}^{(s)} - \mu_{\mathrm{w}}^{(s)}$ and $\phi^{(s)} = \mu_{\mathrm{b}}^{(s)}/\mu_{\mathrm{w}}^{(s)}$. The posterior distributions provide complete uncertainty quantification, from which we extract posterior means and 95% credible intervals for both parameters and test statistics.

Furthermore, to quantify the strength of evidence for group differences, we compute the Bayes Factor comparing the alternative hypothesis against the null hypothesis:

$$BF_{10} = \frac{p(\mathbf{d} \mid H_1)}{p(\mathbf{d} \mid H_0)} \tag{8}$$

Table 2. Statistical comparison across biomarker groups. Permutation testing misses amyloid differences ($p = 0.228$) but detects tau differences ($p = 0.041$), whereas Bayesian analysis provides decisive evidence for topological differences in both cases.

Method	**Statistic**	**A+ vs A-**	**T+ vs T-**
Permutation Test	Observed ϕ	1.103	1.369
	p-value	0.228	0.041
	Decision	Not Sig.	Significant
Bayesian Ratio (ϕ)	Posterior Mean	1.104	1.368
	95% CI	[1.054, 1.157]	[1.299, 1.440]
	$P(\phi > 1)$	1.000	1.000
Bayesian Diff. (Δ)	Posterior Mean	5.976	20.389
	95% CI	[3.160, 8.956]	[16.723, 24.102]
	$P(\Delta > 0)$	1.000	1.000
Bayes Factor	BF_{10} (LOO)	3.25×10^6	1.12×10^{36}
	Interpretation	Decisive for H_1	Decisive for H_1

The Bayes Factor is computed via leave-one-out cross-validation: $\log BF_{10} = \mathrm{elpd}_{H_1} - \mathrm{elpd}_{H_0}$. Following Jeffreys [13], $BF_{10} > 10$ and > 100 indicate strong and decisive evidence for H_1, respectively. Conversely, $BF_{10} < 1$ indicate moderate evidence for H_0, with $BF_{10} < 0.1$ denoting strong evidence for the null. Unlike the frequentist p-values, Bayes factors continuously quantify the strength of evidence for both hypotheses.

Simulation-Based Validation To validate the equivalence between the Bayesian framework and permutation testing, we conducted simulation experiments under two cases using modular networks with $n = 24$ nodes generated via stochastic block models: networks with different structures (c=2 vs c=3) and networks with identical structures (c=3 vs c=3), with 10 networks per group. While real brain networks may exhibit varying degrees of similarity, these conditions allow us to assess the framework's ability to correctly identify both presence and absence of topological differences [2]. Connection probabilities were $p_{\text{within}} = 0.7$ and $p_{\text{between}} = 0.1$, and permutation testing used 5,000 transpositions while Bayesian models employed MCMC with 4 chains and 8,000 draws. As shown in Table 1, both methods are statistically consistent: for different structures, permutation test yielded $p < 0.001$ and Bayesian analysis gave $P(\phi > 1) = 1.000$ with decisive evidence; for identical structures, both correctly identified no significant difference ($p = 0.634$, $P(\phi > 1) = 0.330$), with Bayes factor uniquely quantifying moderate evidence for the null hypothesis.

3 Application to Alzheimer's Disease

Amyloid-beta and tau represent the core pathological hallmarks of Alzheimer's disease [15]. Understanding how these biomarkers differentially affect brain net-

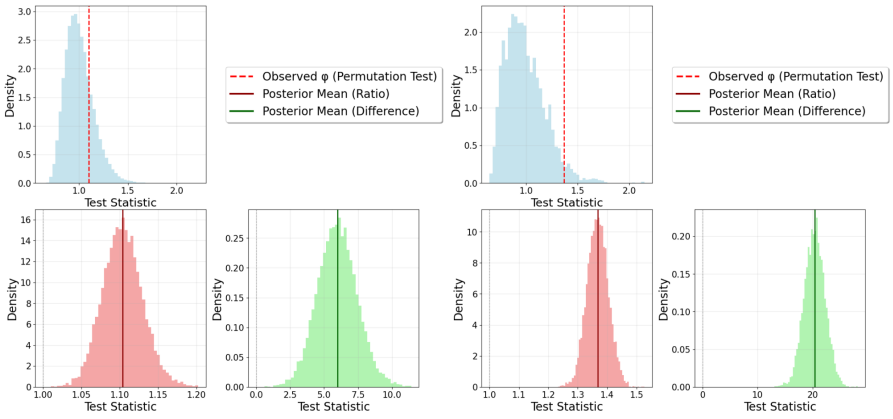

Fig. 1. Comparison of permutation testing and Bayesian inference for Amyloid (left) and Tau (right) groups. In each panel, the top row shows the permutation null distribution (blue) and observed ϕ (red dashed line). The bottom row displays the posterior distributions for the ratio ϕ (red) and difference Δ (green).

work topology is critical for early detection and intervention strategies. We applied our framework to resting-state fMRI data from the Duke/UNC Alzheimer's Disease Research Center (ADRC). The study cohort comprised 167 cognitively unimpaired participants (aged 28.0–80.0 years), stratified via the AT(N) framework for amyloid (34 A+, 133 A-) and tau (20 T+, 147 T-) analyses. The fMRI data were preprocessed using fMRIPrep with standard preprocessing steps, and brain networks were constructed using the AAL atlas (116 regions), with edge weights given by the Pearson correlation coefficients between the mean regional BOLD time series.

Alzheimer's disease biomarkers including beta amyloid 42/40 and phosphorylated tau 181 (pTau-181) were tested using the Simoa® assay platform on a Quanterix™ HD1 instrument housed in the UNC HIV Cure Center and operated by trained Biomarker Core staff. Amyloid positivity (A+) status was determined if the Ab42/40 ratio was ≤ 0.058 and tau positivity (T+) status was determined if pTau-181 was > 63.

Based on these thresholds aligned with the biological AT(N) framework [15], participants were stratified into two primary comparison groups: A+ versus A-, and T+ versus T-. For cognitively unimpaired individuals, A+ status signifies the preclinical stage of AD, marking the earliest pathological changes, while T+ is closely associated with subsequent neurodegeneration and eventual cognitive decline. The connectivity matrices were age-adjusted [4] and analyzed using both methods. Results are summarized in Table 2. Figure 1 visualizes the difference between these approaches: permutation testing evaluates the observed statistic against its null distribution under the no-difference hypothesis, while Bayesian methods directly characterizes the posterior distribution of statistics given the

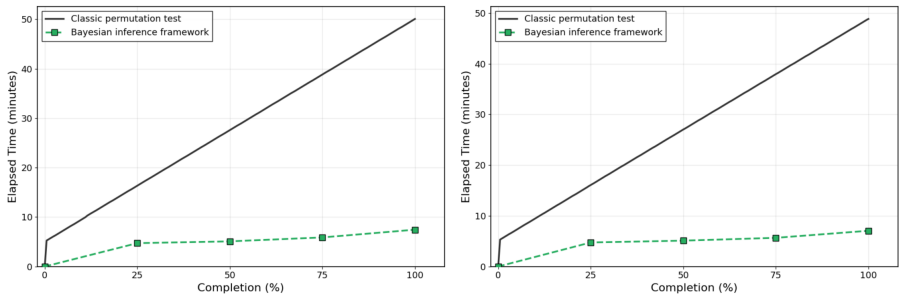

Fig. 2. Computational efficiency comparison. The left panel shows the elapsed execution time for the amyloid-β, and the right panel displays for the tau analysis.

observed data. Additionally, the Bayesian framework provides computational efficiency. As illustrated in Figure 2, unlike permutation tests, whose execution time scales linearly with the number of permutations, the Bayesian approach requires less total execution time, ensuring scalability for large-cohort analyses.

Result For amyloid status comparison, permutation testing yielded $p = 0.228$, failing to detect significant differences at the conventional $\alpha = 0.05$ threshold. In contrast, Bayesian analysis shows $\phi = 1.104$ (95% CI: [1.054, 1.157]) with $P(\phi > 1) = 1.000$ and $\text{BF}_{10} = 3.25 \times 10^6$, providing decisive evidence for group differences. The magnitude of these Bayes factors results from the multiplicative accumulation of pointwise predictive densities during LOO-CV, reflecting strong evidence in favor of H_1.This demonstrates the framework's enhanced sensitivity to subtle network alterations: the method detects approximately 10% increase in between-group dissimilarity ($\phi = 1.104$) and nearly 6-unit absolute difference ($\Delta = 5.976$) that threshold-based testing completely misses. Such sensitivity is particularly valuable for early-stage pathology like amyloid accumulation, where network changes are modest but may carry important clinical implications for disease progression.

For tau status comparison,permutation testing yielded $p = 0.041$, achieving significance at the conventional $\alpha = 0.05$ threshold. Bayesian analysis provides substantially stronger evidence with $\phi = 1.368$ (95% CI: [1.299, 1.440]), $P(\phi > 1) = 1.000$, and $\text{BF}_{10} = 1.12 \times 10^{36}$. Notably, the tau effect is substantially larger than amyloid: $\phi = 1.368$ versus 1.104 represents 37% versus 10% increases in between-group dissimilarity, while $\Delta = 20.389$ versus 5.976 shows a massive difference in distance. This quantitative pattern is consistent with neuroscience literature indicating tau pathology, as a later-stage process, produces more severe functional network disruption than early amyloid accumulation.

Sensitive Analysis While our primary pairwise framework provides a granular characterization of network topologies, we acknowledge a statistical limitation:

Table 3. Results of the patient-level sensitivity analysis. Bayesian framework confirms decisive topological alterations in the T+ group while reflecting the subtle, pre-clinical nature of the A+ group.

Method	**Statistic**	**A+ vs A-**	**T+ vs T-**
Permutation Test	Observed ϕ	1.103	1.369
	p-value	0.288	0.049
	Decision	Not Sig.	Significant
Bayesian Ratio (ϕ)	Posterior Mean	1.087	1.321
	95% CI	[0.960, 1.225]	[1.169, 1.488]
	$P(\phi > 1)$	0.902	1.000
Bayesian Diff. (Δ)	Posterior Mean	4.958	18.299
	95% CI	[-2.534, 12.463]	[10.382, 26.395]
	$P(\Delta > 0)$	0.902	1.000
Bayes Factor	BF_{10} (LOO)	0.172	6530.110
	Interpretation	Moderate for H_0	Decisive for H_1

pairwise distances involving the same individual are inherently correlated. To address this dependence and validate our findings, we conducted a sensitivity check using a patient-level summary approach. By averaging the within-group and between-group distances for each subject ($S_i^{\text{within}} = \frac{1}{m-1}\sum_{k\neq i}\tilde{W}_{\text{top}}(X_i, X_k)$ and $S_i^{\text{between}} = \frac{1}{n}\sum_{l=1}^{n}\tilde{W}_{\text{top}}(X_i, Y_l)$), we mitigated the dependence problem and re-evaluated the topological differences without statistical inflation.

The results are presented in Table 3. These findings demonstrate the robustness of our framework, as the T+ group continued to yield decisive evidence for topological disruption. For the A+ group, the conservative model yielded moderate evidence for the null hypothesis, reaching a conclusion consistent with the classical permutation test. This highlights the biological reality that early-stage amyloid-driven network alterations are subtle. While our primary pairwise model offers the sensitivity required to flag these subtle changes, the conservative sensitivity check indicates that definitively confirming such subtle topological shifts will require substantially larger clinical cohorts.

Discussion This approach complements existing neuroimaging research by moving beyond the binary rejection rules of frequentist methods. Instead, it yields complete posterior distributions of test statistics and provides Bayes factor-based decision criteria, offering richer probabilistic information for clinical interpretation.

Confirming subtle topological changes in early preclinical stages without statistical inflation requires validation on larger clinical cohorts. Future work will extend this approach to region-specific topological networks [8] using Bayesian hierarchical models [7]. In univariate analyses, hierarchical structures act as shrinkage estimators, pulling noise-driven estimates toward the population mean to control false positive rates without depleting statistical power. Furthermore,

adopting a multilevel approach will model the inherent correlations within pairwise network distances, simultaneously addressing the multiple comparisons problem and the data dependency issue.

Compliance with Ethical Standards The ADRC study is approved by the Duke University and University of North Carolina at Chapel Hill institutional review boards in accordance with ethical principles and applicable regulatory requirements (Duke University IRB Protocol Number: Pro00103958). Written informed consent is obtained from all participants ages 25 to 80 years.

Acknowledgments. Research reported in this publication was supported by Duke Science and Technology LAUNCH grant, Bass Connections at Duke University, and the National Institute on Aging of the National Institutes of Health under Award Number P30AG072958.

Disclosure of Interests. The authors have no competing interests to declare that are relevant to the content of this article.

References

1. Alali, M., Imani, M.: Bayesian topology inference of regulatory networks under partial observability. Results in Control and Optimization **19**, 100570 (2025). https://doi.org/10.1016/j.rico.2025.100570
2. Bullmore, E., Sporns, O.: Complex brain networks: Graph theoretical analysis of structural and functional systems. Nature Reviews Neuroscience **10**(3), 186–198 (2009)
3. Carrière, M., Cuturi, M., Oudot, S.: Sliced Wasserstein kernel for persistence diagrams. In: Precup, D., Teh, Y. (eds.) Proceedings of the 34th International Conference on Machine Learning. Proceedings of Machine Learning Research, vol. 70, pp. 664–673. PMLR (2017)
4. Damoiseaux, J.: Effects of aging on functional and structural brain connectivity. Neuroimage **160**, 32–40 (2017)
5. Edelsbrunner, H., Harer, J.: Computational Topology: An Introduction. American Mathematical Society (2022)
6. Edelsbrunner, H., Letscher, D., Zomorodian, A.: Topological persistence and simplification. Discrete & Computational Geometry **28**, 511–533 (2002)
7. Gelman, A., Hill, J., Yajima, M.: Why we (usually) don't have to worry about multiple comparisons. Journal of Research on Educational Effectiveness **5**(2), 189–211 (2012). https://doi.org/10.1080/19345747.2011.618213
8. Greicius, M., Srivastava, G., Reiss, A., Menon, V.: Default-mode network activity distinguishes alzheimer's disease from healthy aging: evidence from functional mri. Proceedings of the National Academy of Sciences **101**(13), 4637–4642 (2004)
9. He, P., Songdechakraiwut, T.: Imaging the topology of dynamic brain connectivity. arXiv preprint arXiv:2511.09949 (2025)
10. Heckerman, D.: A tutorial on learning with bayesian networks. In: Learning in graphical models, pp. 301–354 (1998)
11. Hoff, P.: A first course in Bayesian statistical methods. Springer (2009)

12. Holmes, A., Blair, R., Watson, J., Ford, I.: Nonparametric analysis of statistic images from functional mapping experiments. Journal of Cerebral Blood Flow & Metabolism **16**(1), 7–22 (1996)
13. Jeffreys, H.: The theory of probability. OUP Oxford (1998)
14. Kass, R., Raftery, A.: Bayes factors. Journal of the American Statistical Association **90**(430), 773–795 (1995)
15. Knopman, D., Amieva, H., Petersen, R., Chételat, G., Holtzman, D., Hyman, B., Nixon, R., Jones, D.: Alzheimer disease. Nature Reviews Disease Primers **7**(1), 33 (2021)
16. Ma, Z., Hanson, T.: Bayesian nonparametric test for independence between random vectors. Computational Statistics & Data Analysis **149**, 106959 (2020). https://doi.org/10.1016/j.csda.2020.106959
17. Nichols, T., Holmes, A.: Nonparametric permutation tests for functional neuroimaging: a primer with examples. Human Brain Mapping **15**(1), 1–25 (2002)
18. Shi, S., Bottegal, G., Van den Hof, P.: Bayesian topology identification of linear dynamic networks. CoRR **abs/1903.06205** (2019)
19. Songdechakraiwut, T., Chung, M.: Topological learning for brain networks. The Annals of Applied Statistics **17**(1), 403 (2023)
20. Songdechakraiwut, T., Krause, B.M., Banks, M.I., Nourski, K.V., Van Veen, B.D.: Wasserstein distance-preserving vector space of persistent homology. In: International Conference on Medical Image Computing and Computer-Assisted Intervention. pp. 277–286. Springer (2023)
21. Yi, L., Lutz, M., Wu, Y., Li, Y., Songdechakraiwut, T.: Topological and geometric signatures of brain network dynamics in Alzheimer's disease. Alzheimer's & Dementia **21**(8), e70545 (2025). https://doi.org/10.1002/alz.70545